

Modeling Sulfur-Nitrogen Chemistry inside a Claus Reaction Furnace

Joseph Smith[‡], Ahti Suo-Anttila[§], Vikram Sreedharan[‡], Zach Smith[‡],

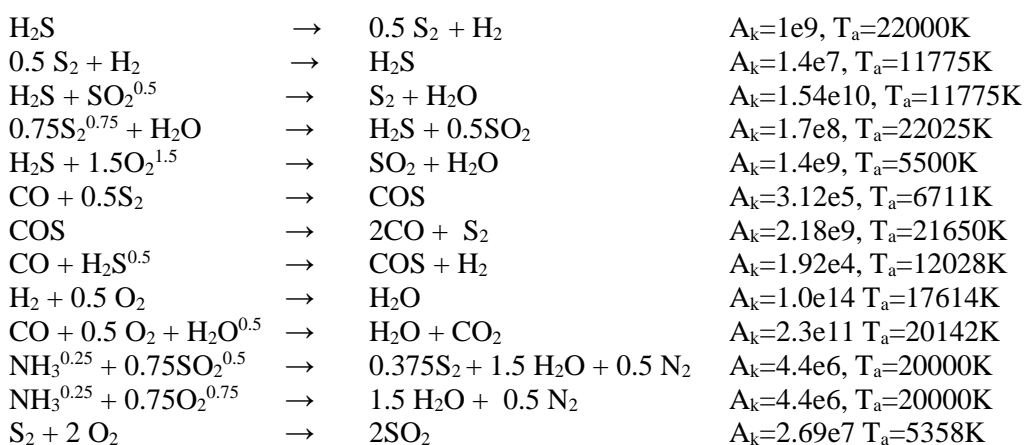
[‡]Chemical and Biochemical Engineering, Missouri Univ of Sci and Tech, Rolla, MO 65409 USA

[§]Computational Engineering Analysis LLC

[‡]Elevated Analytics Consulting, Provo, UT 84770 USA

ABSTRACT

This paper describes a CFD analysis of a Sulfur Recovery Unit (SRU) considering transient turbulent reacting flow inside the SRU. Often, the SRU feedstock includes hydrocarbons together with nitrogen and sulfur species, which react with oxygen in the air to form various emissions including SO₂, NH₃ and NO₂. This work used an LES based CFD code (C3d) to analyze the SRU performance for various feed conditions. This work includes detailed chemical reactions with transient fluid mixing to provide time-accurate results. The complex SRU reaction chemistry described by Ibrahim, et.al. 2020 [1] was simplified based on previous work by Sebbar et.al. (2018) [2] and Andoglu, et.al. (2019) [3] to integrate detailed kinetics with transient fluid flow. Since the SRU feedstock involves hydrocarbons reacting with air, a previously validated C3d combustion model accurately describes the hydrocarbon-oxygen chemistry. The reactions used to describe the nitrogen and sulfur chemistry includes:



Equilibrium reactions were approximated using a combination of forward and reverse reactions. This approach permits the engineering analyses with sulfur and nitrogen species to run on a standard engineering workstation. Predicted results are compared to results from an operating SRU.

INTRODUCTION

Refineries processing high sulfur crude oils generate large quantities of acid gas. Acid gas contains large concentrations of hydrogen sulfide (H₂S) which must not be released into the atmosphere by the refinery. Instead, refineries convert the sulfur components in acid gas into elemental sulfur by the Claus process. The modified Claus process (see Figure 1) is most commonly used by the petrochemical industry to treat acid gas produced in the crude oil refining process. As shown, the Claus process includes several processing units including:

1. Reaction furnace,
2. Inline reheater,
3. Reducing gas generator, and
4. Tail gas incinerator

The reaction furnace (SRU) is the most important step in this process because since this is where most of chemistry involved in converting H₂S into elemental sulfur (S₂ and S₈) occurs. The SRU operates in a reducing condition to restrict SO₂ formation. Liquid sulfur is collected from the condenser and stored (see Figure 2) for shipment via trucks, railcars or ships to end users. Approximately 65 to 70 percent of the sulfur in acid gas is recovered as elemental sulfur.

Hydrogen sulfide conversions between 75% - 80% are common. Computational Fluid Dynamics (CFD) modeling can be used to optimize SRU performance. CFD models rely on reduced kinetic models checked (verified) by comparing predictions with plant data. CFD models typically predict SRU performance within approximately 5% of observed plant performance.

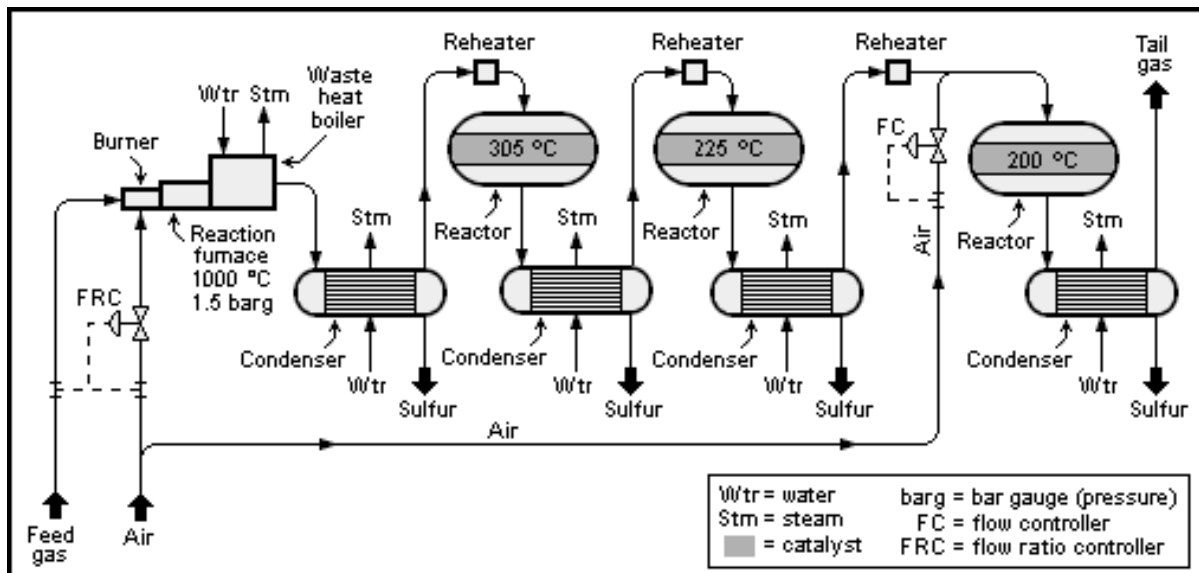


Figure 1 – Process Flow diagram showing the Modified Claus sulfur recovery process.



Figure 2 - Sulfur produced by the Claus process waiting for shipment via ocean vessel

The reaction chemistry occurring in the SRU is further complicated by the ammonia in the acid gas. Nitrogen in the ammonia adds extra reactions that must be included in the reduced kinetic mechanism used in the CFD model to accurately simulate SRU performance.

This paper describes CFD work done to simulate SRU performance with nitrogen and sulfur chemistry in the reaction furnace. Flame shape, reaction temperature, local velocity profile and gas species formed in the SRU are predicted and reported in this paper. Previous work by the authors focused on the second process unit, the inline reheater [4] which heats the acid gas by mixing it with hot reducing products of combustion. If the combustion products being mixed with the acid gas has any oxygen slip, the H_2S will be oxidized into other undesirable compounds including SO_2 and H_2SO_4 that will damage the environment.

The specific focus of this work is to present a reduced chemical kinetic reaction model that has been implemented in our proprietary transient LES based CFD model called C3d. This reaction set and CFD model has been used to simulate a generic SRU unit (see Figure 3) described in our second paper focused on thermal-acoustic coupling inside an SRU.

REACTION CHEMISTRY MECHANISM

The chemistry occurring inside the SRU is very complex and has been modeled using both simplified and detailed chemical kinetic mechanisms models. To simulate the turbulent fluid mixing inside the SRU together with the complex chemical reactions simultaneously, a simplified

set of reactions is used to limit both the memory required to store all the information produced during the simulation and limit the required CPU cycles involved in the simulation to a minimum. For each chemical species included in the calculation, a unique species conservation equation must be solved. Detailed chemical reaction mechanisms (i.e., GRI-mech or others¹) involve hundreds of species and reactions. For full turbulent reacting flow simulations, using a detailed reaction mechanism would overwhelm the capabilities of a typical engineering workstation. Instead, reduced mechanisms have been developed for specific applications such as SRU chemistry.

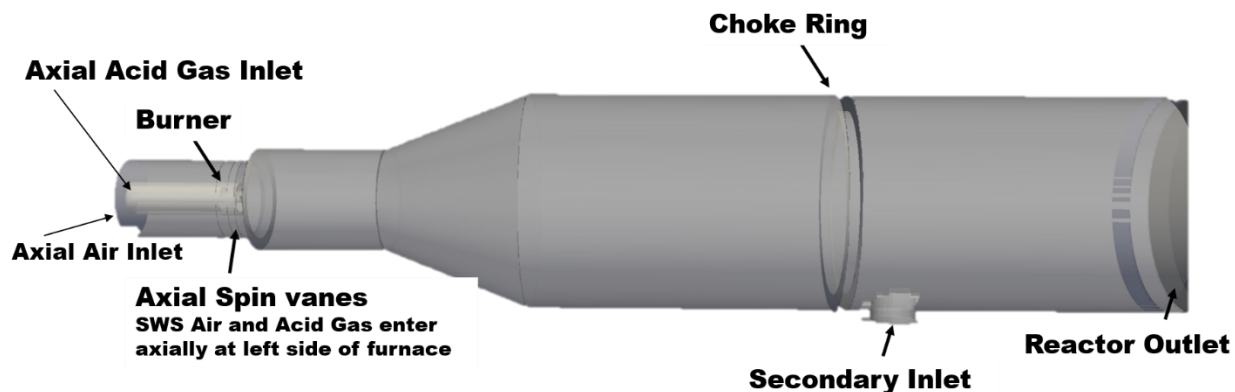
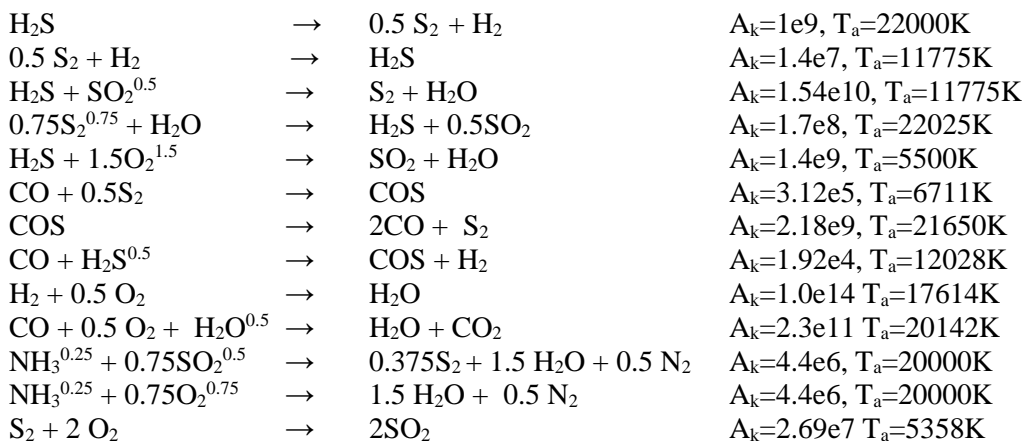


Figure 3 – Generic SRU unit used to convert Acid Gas to elemental sulfur

SRU feedstock typically contain a wide range of hydrocarbons together with nitrogen and sulfur containing compounds. Previous validated C3d combustion modeling of hydrocarbon/oxygen (air) systems that includes hydrocarbon-oxygen chemistry is the starting point for this work. Using the SRU chemistry described by Andoglu [3], Nimmo et al. (1998) [5], Dogru et al. (2018) [6], Karan et al. (1999) [7] and others to augment the previous validated hydrocarbon combustion chemistry in C3d, the following reduced kinetic mechanism of chemical reactions to model SRU chemistry was developed:



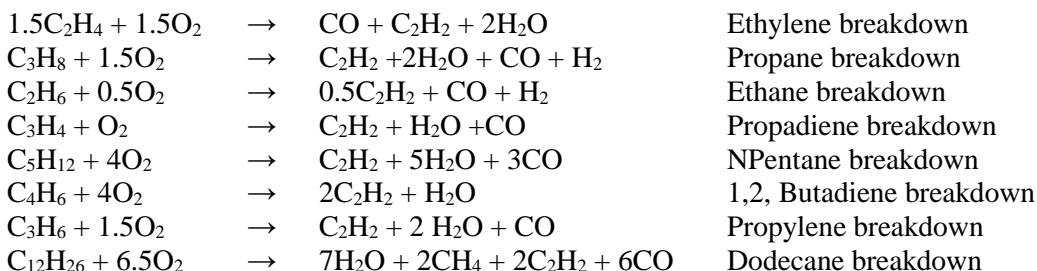
¹ For the latest reaction mechanisms related to methane oxidation, see <http://combustion.berkeley.edu/gri-mech/>; For a more general collection of hydrocarbon combustion chemistry, see: <https://prime.cki-know.org/>

Where equilibrium reactions are described by a combination of forward and reverse reactions. The exponents on the left-hand side of the global reaction equations are the powers that the mole fractions are raised to when solving for reaction rates. It has been shown that the overall decomposition reaction has a first-order dependency on H₂S concentrations in the temperature range of 800°C to 1250°C as described by Karan et al. (1999) [7]. One of the key reactions in the front-end furnace is between H₂S and SO₂. This reaction was studied at actual Claus plant reaction furnace temperatures and residence times by Monnery et al. (2000) [8], and they used the new kinetic data to develop a new reaction rate expression.

The next section describes the hydrocarbon – oxygen combustion reactions, previously validated and described in the C3d combustion model white paper [9].

C3D Hydrocarbon-Oxygen Reaction model.

The C3d combustion model consists of both primary and secondary reactions.² Primary Fuel Breakdown reactions shown below have been used successfully for a wide range of combustion simulations. These reactions can be used individually or combined into a single fuel breakdown reaction by applying mole weighting and adding the mole fraction weighted reactions together to form a mixed fuel type:



Other hydrocarbons not in the list can be added by breaking down the hydrocarbon into CO, C₂H₂, H₂ and H₂O. The various coefficients of breakdown products can be estimated following a few simple rules: 1) Heavy sooting hydrocarbons produce more C₂H₂ and possibly a small amount of soot, 2) The heat release for primary fuel breakdown can be adjusted by producing more H₂O for higher heat release vs. more H₂ for less heat release, 3) The balance of oxygen consumption, and CO production are determined by the elemental balance. It turns out that this combustion model has mild sensitivity to the primary breakdown reactions, which gives the user a lot of flexibility in modeling combustion of various fuels, while the secondary reactions mostly determine the flame temperature and soot production.

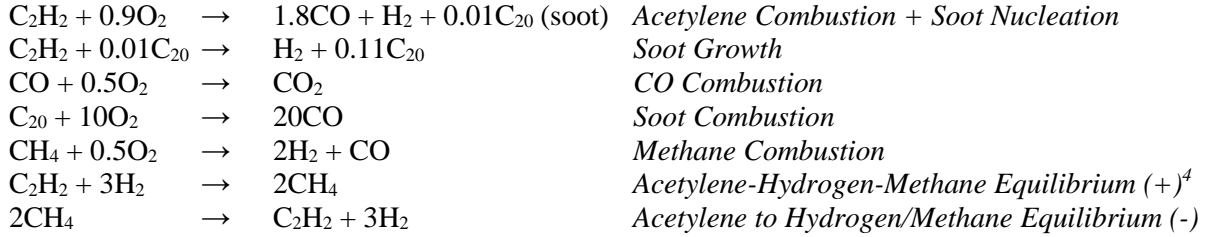
Secondary reactions (after breakdown of primary fuels)

The secondary reactions used in all simulations reported here³ have been calibrated against test data (where available) and do not change from simulation to simulation and are grid independent.

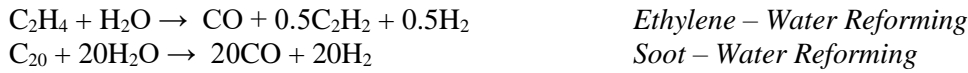


² A complete listing of the combustion reactions will be deferred until after the SRU reactions are described.

³ All of the reaction coefficients shown above are molar values.



In conditions of low oxygen and high temperature, hydrocarbon and soot reforming reactions occur. The reforming reactions are especially important in the central rows of a large ground flare where there is low oxygen within the flame zone because the outer rows have consumed most of it. The primary fuel breakdown reactions produce H^+ and OH^- radicals which are modeled as water vapor (H_2O) – similar to the approach used by Westbrook and Dryer. The reason that water vapor is used as the oxidizing agent is because measurements indicate that actual mole fractions of OH^- and H^+ radicals are on the order of 1% or less, so they are present as trace quantities even though they are the primary reactive species. The water vapor can react both with primary fuel to produce C_2H_2 , CO , and H_2 . It can also oxidize soot to produce CO and H_2 . Thus, typical reforming reactions for ethylene would be:



A global Arrhenius rate model is used for all reactions. As such, the consumption of fuel, soot, and intermediate species are described by:

$$Rate \left(\frac{mol}{s-m^3} \right) = \frac{df_{R_i}}{dt} = -C [\prod_i^N f^{p_{R_i}}] T^B e^{-T_A/T} \quad (1)$$

In this expression, N is the number of reactants. The moles of each reactant for $i = 1$ to N , C is the pre-exponential coefficient for the reaction, and T_A is the effective activation temperature for the reaction and B is a temperature exponent. The activation temperature T_A is simply the activation energy divided by the universal gas constant. The exponent p on the molar concentration allows the use of a global reaction rate. A global reaction rate is often used to fit a simpler reaction to multiple reactions and pathways that result in the same reaction products. Although reaction equation 2 is written in terms of molar concentration, internally within the code, it must be solved in terms of mass concentration. The reason is that the number of moles of reactants and products is not a constant during the reaction time step whereas the total mass of reactants and products remains fixed, and this property allows one to make a numerical approximation for the solution. We see that the local rate of consumption of the primary reactant increases with the local absolute temperature T and the product of all the local reactant mole concentrations. The primary reactants f_1 and f_2 , the effective activation temperature T_A , the pre-exponential coefficient C , global exponent p , and the temperature exponent B for each reaction are given in Table 1. The values in the table were derived from published values in some cases and by comparisons with experiment in others.

⁴ + means forward reaction, - means reverse reaction

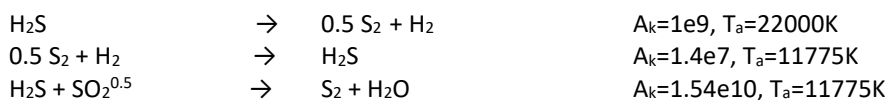
The reactions listed above all obey the normal Arrhenius or global reaction kinetics equation. CO oxidation includes a square root of water mole fraction weighting factor from Westbrook and Dryer. It turns out that the kinetics coefficients for soot oxidation are such that at high enough temperatures where soot oxidation occurs, the reaction rate quickly becomes boundary layer diffusion limited. This is because soot is a particle with a boundary layer, not a gas mixture. The temperature dependence for soot oxidation is due to the variation in mass diffusion coefficient with temperature. Soot oxidation due to water reforming reactions is of higher reactivity than that due to oxygen. Thus, the soot oxidation due to oxygen is less than that for water reforming reactions and furthermore is combined with an eddy breakup time delay because oxygen must diffuse into the flame zone from outside.

Table 1 - Arrhenius Reaction Coefficients for a Typical Hydrocarbon Fuel Fire

| Reaction | f_1 | f_2 | T_A (K) | C (1/s) | B |
|--|-------------------|----------------------------|--------------|--------------|------|
| Primary Fuel Breakdown (ethylene) | $[C_2H_4]^{0.1}$ | $[O_2]^{1.65}$ | 0 K | 1 | 2 |
| Hydrogen Combustion | $[H_2]^{0.33}$ | O_2 | 10000 K | 1e8 | 0 |
| Acetylene combustion & soot nucleation | $[C_2H_2]^{0.33}$ | O_2 | 15110 K | 2e8 | 2 |
| Acetylene + soot growth | $[C_{20}]^{0.33}$ | C_2H_2 | 15110 K | 1e7 | 0 |
| CO – Oxygen combustion | CO | $[O_2]^{0.25}[H_2O]^{0.5}$ | 20142 K | 1e18 | 0 |
| Soot combustion | $[C_{20}]^{0.33}$ | O_2 | 0 K | 0.5 | 0.75 |
| Methane combustion | CH_4 | O_2 | 15000 K | 1e12 | 0 |
| Forward Acetylene – Hydrogen – Methane | C_2H_2 | H_2 | 15110 K | 5e7 | 0 |
| Reverse Acetylene – Hydrogen - Methane | CH_4 | CH_4 | 23500 K | 4e9 | 0 |
| Ethylene - Water Reforming | C_2H_4 | H_2O | 15000 K | 5e6 | 0 |
| Soot – Water Reforming | $[C_{20}]^{0.1}$ | $[H_2O]^{1.7}$ | 0 K | 1.0 | 0.75 |

Derivation of H₂S and SO₂ Reaction Kinetics

The derivation of H₂S and SO₂ reaction parameters relies upon comparisons to experiment and theory. Many others have published values for reduced reactions sets of H₂S and SO₂ chemistry. However, when using published reaction parameters comparisons with experiments often leads to disappointing results. As a result, reaction parameters for the first 4 reactions were independently derived in this work. The first 4 reactions are:





The methodology of derivation is as follows.

The first step is to assume that the temperature dependence in the exponential term of the kinetics equations published by others is correct. That is the activation temperature values are not modified and are assumed correct.

H₂S chemistry includes both Arrhenius breakdown and recombination. To derive appropriate pre-exponential values a two-step procedure was adopted. Since both forward and reverse reactions are involved the ratio of the pre-exponential terms can be obtained from equilibrium values at a specified temperature. To this end the NASA CEA (Chemical Equilibrium with Applications) website was used. An initial 99.8% H₂S – 0.2% air mixture at 1300K was input to yield an equilibrium mass fractions of H₂=0.0128, H₂S=0.78, S₂=0.2. The pre-exponential coefficients were adjusted to give the same results as shown in the Figure 4 below.

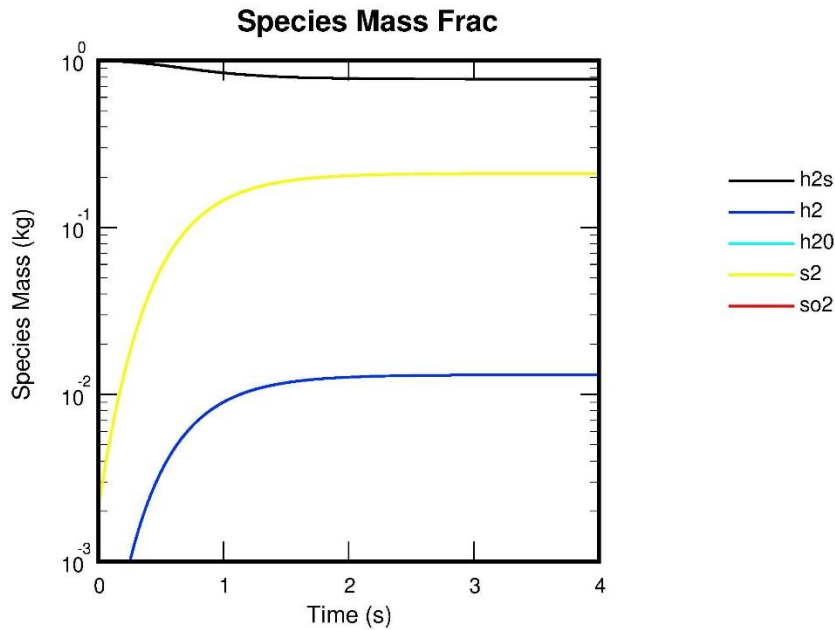


Figure 4 - Predicted mass fractions of reactants for H₂S equilibrium at 1300K

The predicted equilibrium values are within a few percent of the NASA predicted values. The pre-exponential values are in the correct ratio (forward/reverse ratio = 526), but the kinetic rate cannot be determined from equilibrium values. To get the kinetic rate the experimental data of Monnery et. al. (2000) [8] was used. They quote a value of 80% to equilibrium for a 3% mixture of H₂S - N₂ at 1423K. The pre-exponential values were adjusted to give those measured results while keeping the ratio of forward to reverse as before (526). The final adjusted values were used in generating the predictions shown in Figure 4.

The next step in Claus chemistry is to add SO_2 to the mixture. A mixture of H_2S and SO_2 has both H_2S equilibria reactions and $\text{SO}_2 + \text{H}_2\text{S} = \text{S}_2 + \text{H}_2\text{O}$ equilibrium reactions. So, it is significantly more complicated than the H_2S alone equilibrium. The same procedure was followed to establish the forward and reverse pre-exponential values for the $\text{SO}_2 + \text{H}_2\text{S}$ reactions. The previously derived values for H_2S equilibria were used and SO_2 reactions were added, giving a total of 4 chemical reactions. The NASA CEA values for 50-50 wt % mixture of $\text{H}_2\text{S} + \text{SO}_2$ results in $\text{H}_2\text{O}=0.19$, $\text{H}_2\text{S}=0.11$, $\text{SO}_2=0.15$, $\text{S}_2=0.5$, $\text{H}_2=0.001$, at 1300K. Figure 5 shows the predicted results.

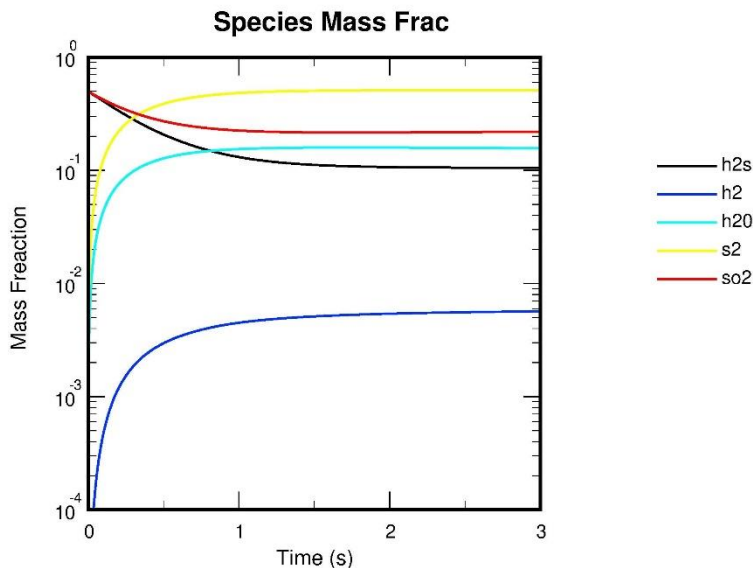


Figure 5 - Predicted mass fractions for an initial mixture of 50-50 wt% $\text{H}_2\text{S} + \text{SO}_2$ at 1300K

As shown in Figure 5, the agreement is not perfect but is acceptable for use in the Claus CFD analysis given the simplification of the overall chemistry. The kinetics rate data was adjusted based upon the tube reactor data from Monnery et. al. (2000) [8] wherein the fractional approach to equilibrium was reported as 40% for SO_2 mole fraction at 1323K and 0.5 sec in a dilute 3% mixture of SO_2 , H_2S , and N_2 .

Now that $\text{H}_2\text{S} + \text{SO}_2$ chemistry kinetics is known, and agreement with both experiment and theory has been achieved, the combustion of hydrocarbons and NH_3 oxidation reactions can be added to perform overall SRU furnace analysis. The combustion of hydrocarbons was calibrated from a variety of combustion experiments. The NH_3 reactions were not compared to experiment, but the rate coefficients were adjusted so that complete burnup of NH_3 is observed provided sufficient O_2 is available.

RESULTS

A typical reaction furnace is shown in the schematic of Figure 3. An analysis of that type of furnace along with typical flows found in an industrial setting was made using C3d along with the chemistry described in this paper.

Inlet Flows:

| Species | Air | NH ₃ | H ₂ S | CO ₂ | H ₂ O | C ₃ H ₈ |
|------------------|-----|-----------------|------------------|-----------------|------------------|-------------------------------|
| Mass Flow (kg/s) | 40 | 2.4 | 10.7 | 0.03 | 2.9 | 0.08 |

Outlet Flows:

| Species | N ₂ | NH ₃ | H ₂ S | S ₂ | H ₂ O |
|------------------|----------------|-----------------|------------------|----------------|------------------|
| Mass Flow (kg/s) | 26.5 | 0.0 | 3.0 | 5.0 | 10.2 |

The predicted gas temperature and mole fractions of some species are shown in the figures below:

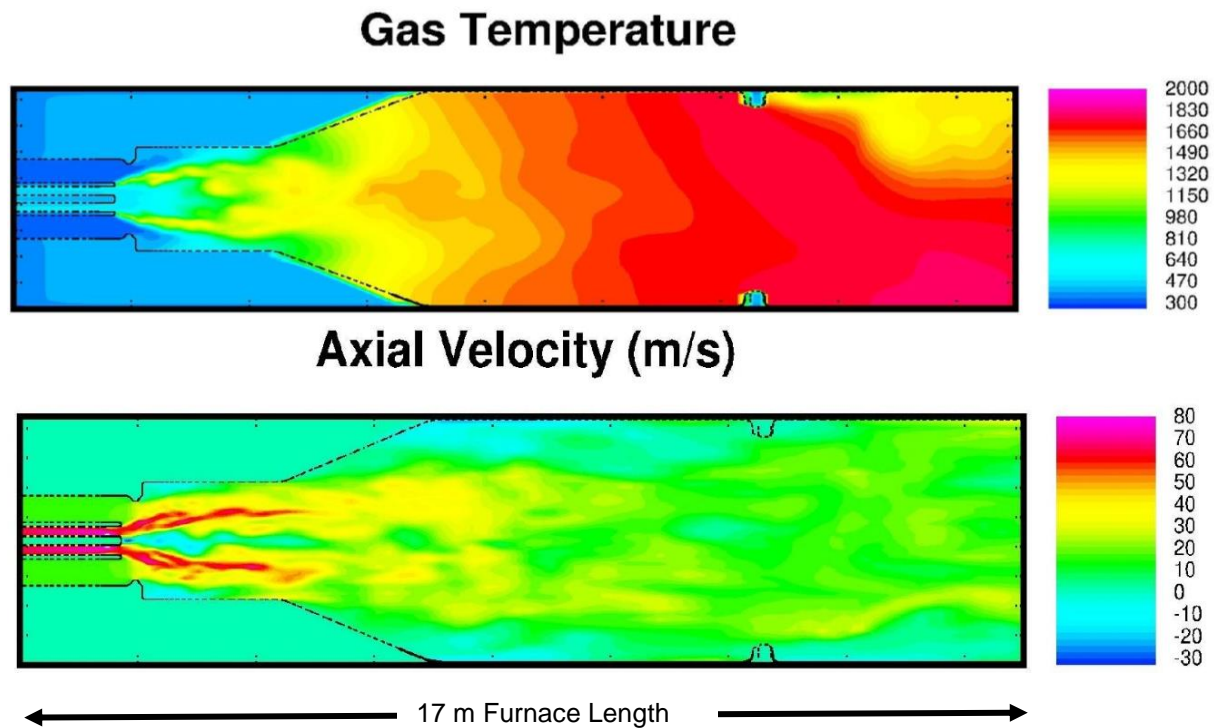


Figure 6 - Predicted gas temperature and velocity centerline profile for the generic SRU reactor

The overall temperature profile (Figure 6) shows an early cooler region where the H₂S is converted to SO₂ and a cooler region just after the choke where propane, fed from a secondary inlet, is oxidized. The centerline velocity profile shows the mixing early in the reactor.

C3H8

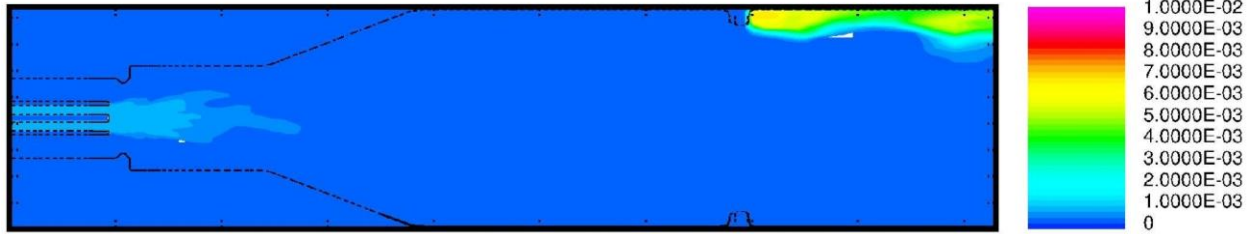
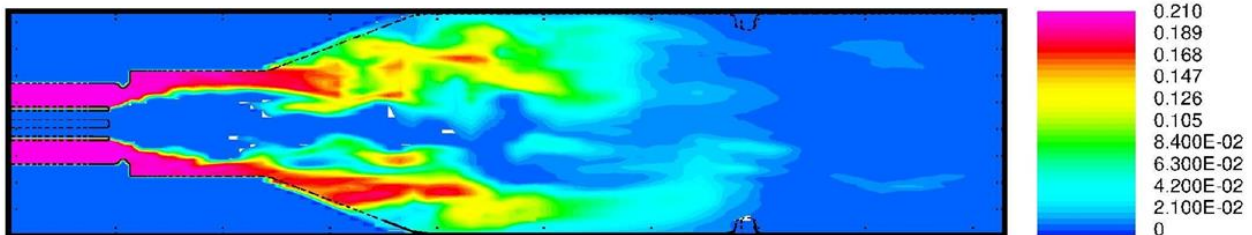


Figure 7 - Predicted propane in generic SRU reactor

Propane, fed as waste gas from the refinery, reacts as part of the primary hydrocarbon-oxygen reactions which leads to the formation of carbon monoxide, water vapor and acetylene. This acetylene is the main precursor to soot formation as illustrated in the list of secondary reactions. However, given the low propane concentration in the fuel stream, acetylene and soot formation are nearly negligible.

The Arrhenius breakdown and recombination of hydrogen sulfide is accompanied by the inclusion of SO_2 in the chemical kinetics model (both forward and backward reactions). The regions of evolution of higher mass fractions of sulfur dioxide and water vapor correspond with higher temperature regions within the reactor. The oxidation of ammonia, hydrogen sulfide and intermediate species result in the evolution of an increase in water vapor toward the end of the reaction furnace as shown in Figure 8.

O2



H2O

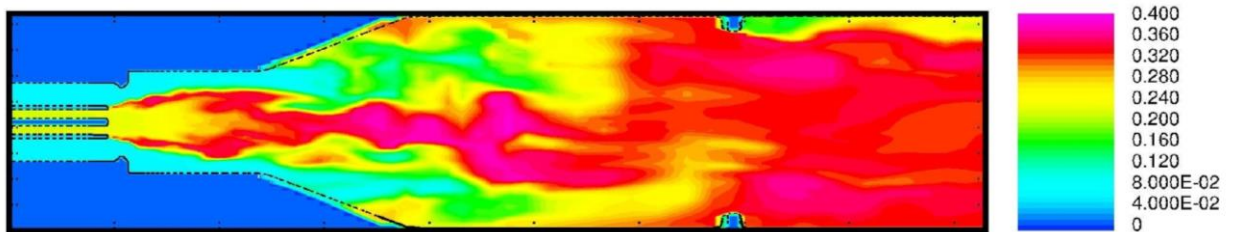


Figure 8 - Centerline concentration profiles for oxygen and water vapor

Hydrocarbon combustion leads to the formation of carbon monoxide and carbon dioxide in the furnace as shown in Figure 9.

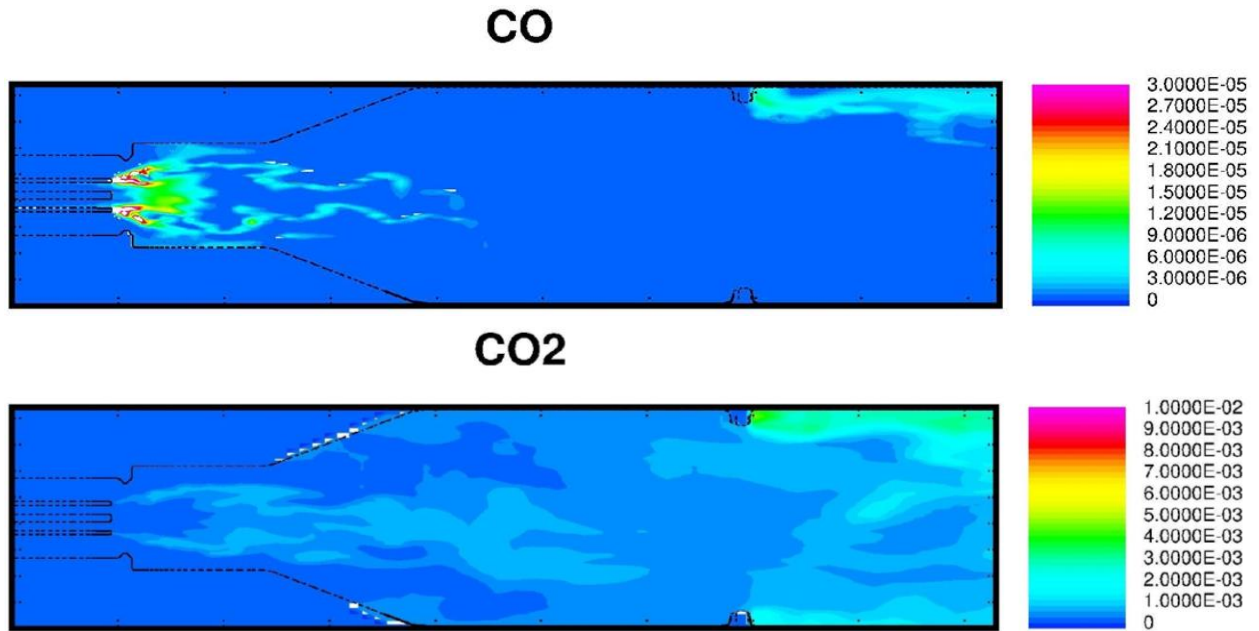


Figure 9 – Centerline concentration profiles of carbon monoxide and carbon dioxide

The formation of elemental sulfur (Figure 10) is driven by both the thermal breakdown of COS and more importantly by the H₂S and SO₂ reaction (Figure 11).

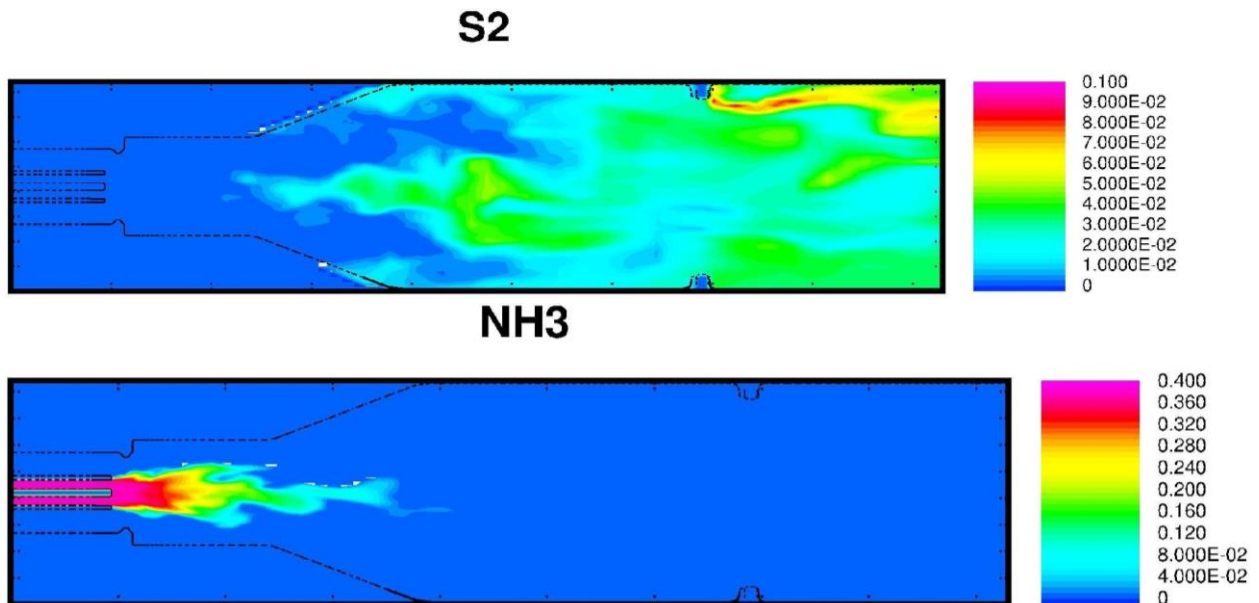


Figure 10 - Centerline concentration profiles of ammonia and elemental sulfur

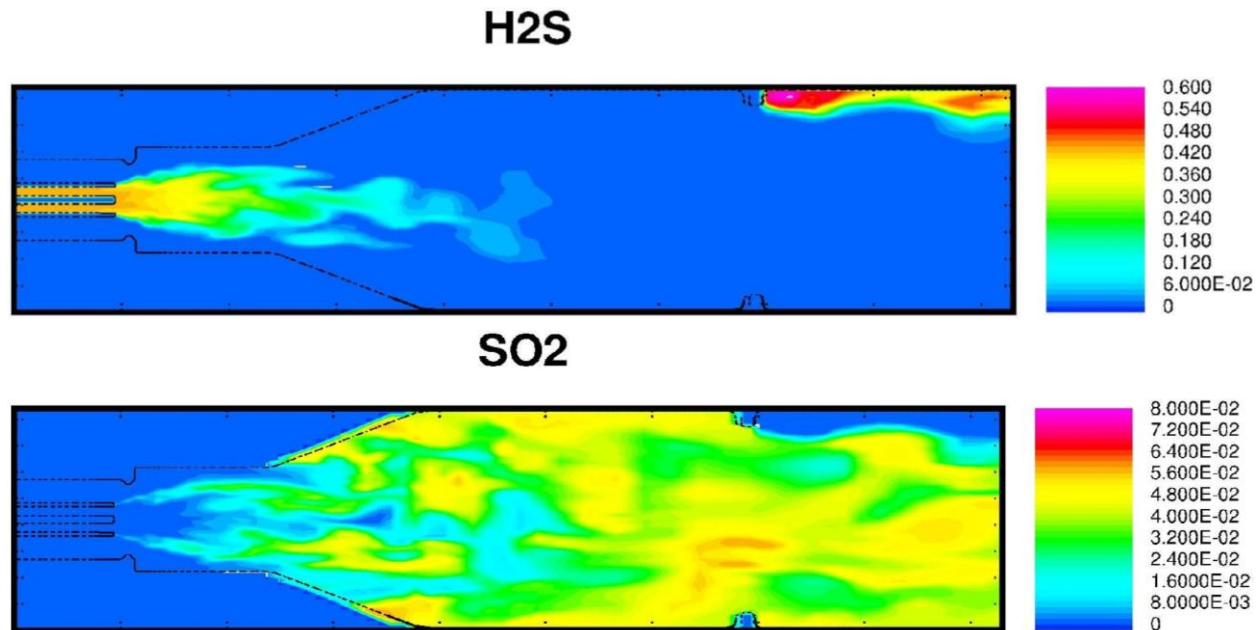


Figure 11 - Centerline profiles of hydrogen sulfide and sulfur dioxide

CONCLUSIONS

The results shown above utilize a global chemical kinetic reaction mechanism involving both sulfur and nitrogen chemistry together with standard hydrocarbon combustion chemistry. Soot production is also included in this mechanism. This work was done to illustrate the ability to include kinetic rates with transient turbulent combustion inside an industrial scale reactor. Although these results are based on a fictitious case, they illustrate the ability to develop and use the reduced mechanism capable to predict sulfur and nitrogen chemistry together with hydrocarbon combustion in a turbulent, transient reacting system such as that occurring inside an industrial scale SRU. In general, this work showed that:

1. H2S to SO2 fed to a reaction furnace operated within the expected pressure, temperature, and residence time for a typical SRU reaction furnace (130-180 kPa/975-1300°C/0.5-2.0s residence time).
2. Detailed chemistry for sulfur and nitrogen could be added to hydrocarbon combustion chemistry to develop a reduced chemical kinetic mechanism that properly describes the reactions occurring inside the reaction furnace.
3. Turbulent reacting flow described by the reduced chemical mechanism could be used to optimize reaction furnace performance for varying feed rates and compositions.
4. The model described in this paper can be used to evaluate how:
 - a. Air to Acid Gas flow ratio impact (increased Air/AG ratio increases H2 production)
 - b. Effect of inlet air temperature (increased temperature increases sulfur production)
 - c. Reactor Optimization for non-design conditions.

REFERENCES

- [1] S. Ibrahim, M. Al-Hamadi and A. Raj, "A detailed reaction mechanism to predict ammonia destruction in the thermal section of sulfur recovery units," *Ind. Eng. Chem. Res.*, vol. 59, no. 11, p. 4912–4923, 2020.
- [2] N. Sebbar, T. Zirwes, P. Habisreuther, J. W. Bozzelli, H. Bockhorn and D. Trimis, "S₂ + Air Combustion: Reaction Kinetics, Flame Structure, and Laminar Flame Behavior," *Energy & Fuels*, vol. 32, no. 10, p. 10184–10193, 2018.
- [3] E. Andoglua, A. Dell'Angelob, E. Ranzib, S. Kaytakoglu and F. Manentib, "Reduced and Detailed Kinetic Models Comparison for Thermal Furnace of Sulfur Recovery Units," *Chemical Engineering Transactions*, p. 76, 2019.
- [4] J. Smith, M. Henneke, J. Petersen, J. McDonald and D. Wilson, "CFD modeling ensures safe and environmentally friendly performance in Shell Claus Off-Gas Treating (SCOT) Unit," in *AFRC-JFRC 2004 Joint International Combustion Symposium*, Maui, Hawaii, 2004.
- [5] W. Nimmo, E. Hampartsoumian, K. Hughes and A. Tomlin, "Experimental and Kinetic Studies of the Effect of Sulfur-Nitrogen Interactions on NO Formation in Flames," *Twenty-Seventh Symposium (International) on Combustion/The Combustion Institute*, vol. 27th, p. 1419–1426, 1998.
- [6] O. Dogru, B. Guzel, G. IS, G. Kusoglu, M. Yagci, M. Kolbasi, G. Ogur and E. Alper, "Modeling Thermal Part of Sulfur Recovery Unit and Simulation Based Analysis of Effects of Air Temperature on Entire Plant," *Int J Petrochem Res*, vol. 2, no. 3, pp. 223-229, 2018.
- [7] K. Karan, A. Mehrotra and L. Behie, "A high-temperature experimental and modeling study of homogeneous gas-phase COS reactions applied to Claus plants," *Chemical Engineering Science*, vol. 54, no. 15–16, pp. 2999-3006, July 1999.
- [8] K. A. H. A. P. W. Y. S. W. D. Monnery, "New experimental data and kinetic rate expression for the Claus reaction," *Chemical Engineering Science*, vol. 55, no. 21, pp. 5141-5148, 2000.
- [9] A. J. Suo-Anttila, "C3d Combustion Model Validation," ResearchGate (DOI: 10.13140/RG.2.2.18264.32000), Albuquerque, January 2019.